Effect of Nitric Oxide on the Anticancer Activity of the Topoisomerase-Active Drugs Etoposide and Adriamycin in Human Melanoma Cells

Birandra K. Sinha, Ashutosh Kumar, Suchandra Bhattacharjee, Michael G. Espey, and Ronald P. Mason

Laboratory of Toxicology and Pharmacology, National Institute of Environmental Health Sciences, National Institutes of Health, Research Triangle Park, North Carolina (B.K.S., A.K., S.B., R.P.M.); and National Institute of Diabetes and Digestive and Kidney Diseases, National Institutes of Health, Bethesda, Maryland (M.G.E.)

ABSTRACT

Nitric oxide ($^.$NO) was originally identified as an innate cytotoxin. However, in tumors it can enhance resistance to chemotherapy and exacerbate cancer progression. Our previous studies indicated that $^.$NO/$^.$NO-derived species react with etoposide (VP-16) in vitro and form products that show significantly reduced activity toward HL60 cells and lipopolysaccharide (LPS)-induced macrophages. Here, we further confirm the hypothesis that $^{.+}$NO generation contributes to VP-16 resistance by examining interactions of $^.$NO with VP-16 in inducible nitric-oxide synthase (iNOS)–expressing human melanoma A375 cells. Inhibition of iNOS catalysis by N^6-(1-iminoethyl)-L-lysine dihydrochloride (L-NIL) in human melanoma A375 cells reversed VP-16 resistance, leading to increased DNA damage and apoptosis. Furthermore, we found that coculturing A375 melanoma cells with LPS-induced macrophage RAW cells also significantly reduced VP-16 cytotoxicity and DNA damage in A375 cells. We also examined the interactions of $^.$NO with another topoisomerase active drug, Adriamycin, in A375 cells. In contrast, to VP-16, $^.$NO caused no significant modulation of cytotoxicity or Adriamycin-dependent apoptosis, suggesting that $^.$NO does not interact with Adriamycin. Our studies support the hypothesis that $^.$NO oxidative chemistry can detoxify VP-16 through direct nitrogen oxide radical attack. Our results provide insights into the pharmacology and anticancer mechanisms of VP-16 that may ultimately contribute to increased resistance, treatment failure, and induction of secondary leukemia in VP-16–treated patients.

Introduction

Topoisomerases constitute an important class of nuclear enzymes responsible for maintaining the topology and function of DNA. Inhibition and/or interference with topoisomerase functions lead to cell death. A large number of clinically active anticancer drugs (e.g., etoposide, adriamycin, and camptothecin) interact with and poison topoisomerases, causing significant DNA damage and cell death. Etoposide (VP-16), a topoisomerase II (topo II) poison, is active against lung and testicular cancers and lymphoma (Henwood and Brogden, 1990). Adriamycin (Adr), also a Topo II poison (Liu, 1989), is active against a wide range of cancers, including leukemias, bladder, breast, lung, and multiple myelomas (Sinha, 1995).

VP-16 is rapidly metabolized by cytochrome P-450 (P450) and peroxidases to o-dihydroxy and o-quinone derivatives of VP-16 (Haim et al., 1986, 1987a,b; VanMaanen et al., 1987;

Kalyanaraman et al., 1989; Kagan et al., 2001), and the formation of these metabolites requires the generation of a VP-16 radical (VP-16$^.$) formed from the oxidation of the 4′-OH group of VP-16 (Haim et al., 1987a,b). VP-16 metabolites bind to cellular components (Haim et al., 1986, 1987b) and cause DNA strand cleavage through a Topo II–mediated mechanism (Sinha et al., 1990; Gantchev and Hunting, 1998). VP-16$^.$ causes oxidative stress both in vitro and in vivo by oxidizing glutathione and forming the glutathione thiol radical (Katki et al., 1987). In addition, VP-16-o-quinone has been reported to form glutathione adducts in HL60 cells (Fan et al., 2006).

Adriamycin has been reported to intercalate into DNA and binds covalently to DNA and proteins via generation of reactive species through reductive bioactivation (Sinha, 1980; Sinha et al., 1984). Reductive activation also generates free radicals via the formation of semiquinone radical and its reaction with molecular oxygen (Kalyanaraman et al., 1980; Myers et al., 1987; Sinha et al., 1987). Although the covalent binding to DNA and formation of free radicals are implicated in the mechanisms of Adr cytotoxicity (Myers et al., 1987; Sinha et al., 1987) and cardiotoxicity (Doroshow

ABBREVIATIONS: Adr, adriamycin; P450, cytochrome P450; ELISA, enzyme-linked immunosorbent assay; HPLC, high-performance liquid chromatography; iNOS, inducible nitric-oxide synthase; L-NIL, N^6-(1-iminoethyl)-L-lysine hydrochloride; LPS, lipopolysaccharide; MTT, microculture tetrazolium toxicity; $^.$NO, nitric oxide; $^.$NO$_2$, nitrogen dioxide; PBS, phosphate-buffered saline; VP-16, etoposide; VP-16$^.$, VP-16-phenoxyl radical; Topo II, topoisomerase II.

1983; Rajagopalan et al., 1988), poisoning of Topo II is considered to play an important role in tumor cell death.

˙NO and/or its products (˙NO₂, ONOOH) have been shown to play important roles in cancer biology, including the innate immune response, neovascularization, cancer metastasis, and cell death (Jenkins et al., 1995; Wink et al., 1998; Xu et al., 2002; Chen et al., 2008). Exposure to ˙NO (via NO donors) modifies activities of certain anticancer drugs, including Adr (Cook et al., 1997; Wink et al., 1997; Evig et al., 2004). ˙NO and/or its products react with a wide variety of substrates, including amines, thiols, and phenols (Janzen et al., 1993; Cudic and Ducrocq, 2000; Yenes and Messeguer 1999). ˙NO-derived species rapidly react with phenols to form phenoxyl radicals, quinones, and nitrated phenols. The formation of nitrotyrosine in cellular proteins has been associated with modifications of protein activities (Curtis et al., 1996; Chatterjee et al., 2009). Furthermore, ˙NO has been reported to react with the tyrosyl radical of ribonucleotide reductase, resulting in the inhibition of DNA synthesis and ultimately cell death (Lepoivre et al., 1994).

VP-16 contains a phenolic OH group in the 4′-position, and both the cytotoxicity and the binding of VP-16 to Topo II depend on the presence of this moiety (Loike and Horwitz, 1976; Long et al., 1984; Sinha et al., 1990). We have recently shown that the phenolic OH of VP-16 reacts with ˙NO-derived species to generate VP-16˙, o-quinone, and other products, thereby modulating the cytotoxicity of VP-16 toward cancer cells (Sinha et al., 2013). In this report, we have further examined the interactions of VP-16 and Adr with endogenously formed ˙NO via iNOS catalysis in A375 human melanoma cells. Our results support the conclusion that the reaction of ˙NO with VP-16 diminishes its cytotoxic activity toward cancer cells. In contrast, endogenously formed ˙NO in A375 cells had no significant effects on Adr cytotoxicity, indicating that Adr did not interact with ˙NO or ˙NO-derived species. This work extends our in vitro work to the cellular systems and confirms the same processes observed for VP-16 in vitro also operates in tumor cells.

Materials and Methods

VP-16 and Adriamycin were the gift of the Drug Synthesis and Chemistry Branch, Development Therapeutic Program of the National Cancer Institute, National Institutes of Health. Human topoisomerases and SDS/KCl precipitation assay kits were obtained from Topogen (Columbus, OH). The nitric-oxide synthase (inducible, iNOS) inhibitor N^6-(1-iminoethyl)-L-lysine dihydrochloride (L-NIL) was obtained from Cayman Chemicals (Ann Arbor, MI). Caspase-3 activity was measured by an Abcam assay kit (Cambridge, MA). A primary antibody for the analysis of iNOS was obtained from Santa Cruz Biotechnology (Santa Cruz, CA). A nitric oxide assay kit was purchased from Thermo Fisher Scientific (Waltham, MA).

Cytotoxicity Studies. A375 melanoma cell lines and macrophage RAW 264.7 cells [American Type Culture Collection (ATCC), Manassas, VA] were grown in phenol red–free RPMI 1640 media supplemented with 10% fetal bovine serum and antibiotics. A375 cells and RAW 264.7 were used for 15 passages, after which the cells were discarded and a new cell culture was started from fresh-frozen stock.

The intracellular reaction between VP-16 and endogenous ˙NO was examined in A375 cells by preincubating cells either in the presence or absence of an iNOS inhibitor (L-NIL) for 4 hours before the addition of VP-16. A375 cells (2000/well) were plated in phenol red–free medium and cultured for 96 hours. Dimethylsulfoxide was included as the vehicle control, and the cytotoxicity was measured by the microculture

tetrazolium toxicity (MTT) assay, as described elsewhere (Alley et al., 1988).

Coculture experiments for cytotoxicity with A375 cells and induced RAW cells were performed in six-well plates separated by 0.4-μM membrane filters (Costar, Corning, NY). Macrophage RAW cells were induced as described previously elsewhere (Sinha et al., 2013). For the cytotoxicity studies, 200,000–250,000/well of A375 cells were plated in 3 ml of complete medium into a six-well plate (in duplicates) and were allowed to attach for 4–6 hours. Membranes were inserted, and various concentrations of VP-16 were added onto the top of membranes containing cells induced with lipopolysaccharide (LPS) (1×10^6) and incubated for 48 hours. Membranes and RAW cells were removed, A375 cells were washed once with ice-cold phosphate-buffered saline (PBS) and trypsinized, and the cytotoxicity was determined by counting the cells. Nitrite concentrations were determined using the Greiss reagent, as described previously elsewhere (Sinha et al., 2013).

Western Blot Assay. Samples (10 μg of total protein) were electrophoresed under reducing conditions through 4%–12% Bis-Tris NuPage acrylamide gels (Invitrogen, Carlsbad, CA). After electrophoresis, proteins were transferred onto a nitrocellulose membrane and probed with anti-iNOS and anti-β actin antibodies. An Odyssey infrared imaging system (Li-Cor Biosciences, Lincoln, NE) was used to acquire images. Rabbit polyclonal anti-iNOS antibody was used to quantitate iNOS proteins in samples using a standard enzyme-linked immunosorbent assay (ELISA) (Ranguelova et al., 2008).

Caspase-3 Assay. Caspase-3 activity in the A375 cell lysate was measured by a colorimetric assay kit (Abcam) using the manufacturer's instructions. In brief, 1 million cells were treated with VP-16 (25 and 50 μM) in the presence or absence of L-NIL (250–400 μM) for 18 hours. Cells were collected by centrifugation and lysed with the lysis buffer (Abcam) by incubating for 10 minutes on ice. Cells were centrifuged at 10,000g for 5 minutes, supernatant was collected, and the protein concentration was determined by the BCA assay. Equal amounts of the protein (200–400 μg) were incubated with 10 mM DTT (dithiothreitol) containing the reaction buffer, followed by the addition of caspase-3 substrate (DEVD-Pna, 4 mM), and the reaction mixture was incubated at 37°C for 2–4 hours. The sample was analyzed for absorbance at 405 nm in a multiwell plate reader, and results were expressed as substrate utilization per milligram protein.

SDS-KCl Precipitation Assay. The formation of covalent Topo II/DNA complexes with VP-16 in the presence or absence of L-NIL was quantitated by the SDS-KCl precipitation assay, as described elsewhere (Liu et al., 1983). In brief, DNA of A375 cells growing in the logarithmic phase (2×10^6 /ml) was labeled with [methyl-^{3}H]thymidine (10 μci, 2 Ci/mmol; PerkinElmer Life and Analytical Sciences, Waltham, MA) for 18–24 hours. Cells were collected and washed twice with the medium, diluted in fresh medium, and seeded into a six-well plate at a density of 2×10^5 cells/ml. L-NIL was preincubated with the cells for 18 hours during the labeling phase. VP-16, dissolved in dimethylsulfoxide, was added and incubated for 1 hour. Cells were washed with PBS (2 times) and lysed with 1 ml of prewarmed lysis solution (Topogen). After lysis and shearing of DNA, DNA–Topo II–VP-16 complexes were precipitated with KCl. The precipitate was collected by centrifugation and washed extensively (4 times) with the washing solution (Topogen) according to the manufacturer's instructions. The radioactivity was counted in a scintillation counter after adding 5 ml of scintillation fluid.

The effects of endogenously generated ˙NO from iNOS of LPS-induced macrophage RAW cells on SDS-KCl precipitate formation in A375 cells were investigated as described in the cytotoxicity studies, except that the drug exposure was for 90 minutes and the samples were processed for the SDS-KCl precipitation assay as described previously. In some experiments, VP-16 (10 μM) was preincubated with LPS-induced RAW cells (0.5×10^6 cells/ml, 30 minutes), the mixtures were added to six-well plates fitted with membrane filters (on top), and they were allowed to interact with the ^{3}H-labeled A375 cells (in bottom, 200–250,000 cells/well) for 90 minutes. The medium was removed, and the cells were washed once with PBS; A375 cells

were lysed with prewarmed lysis buffer, and the samples were processed as described previously.

Metabolism of VP-16 in A375 Cells. The metabolic studies with VP-16 in A375 cells in the presence and absence of L-NIL were performed similarly to those described previously elsewhere (Haim et al., 1987a,b). In brief, 1×10^6/ml of cells in 5 ml of phenol red-free media were seeded in a 100×15 mm Petri dish (Falcon; Becton Dickinson, Franklin Lakes, NJ) and were allowed to attach for 4 hours. L-NIL (400 μM) was added to the cells and incubated for 18 hours before VP-16 (100 μM) was added at various time points. At the end of the incubation, the cells were washed with ice-cold PBS (5 ml), gently scraped in 5 ml of ice-cold PBS, and collected by centrifugation (2000g, 5 minutes). The cells were suspended in 1 ml of ice-cold PBS, lysed with sonication (4°C), and the resulting mixture extracted with chloroform (4 × 1 ml). The combined organic layers were removed under argon, and the residue was dissolved in 200 μl of methanol and analyzed by high-performance liquid chromatography (HPLC) as described previously elsewhere (Haim et al., 1987a,b), except that a C18 column was used and MeOH-water (60:40) was the mobile phase. Under these conditions, VP-16 and VP-16-o-quinone had retention times of 2.1 minutes and 2.7 minutes, respectively.

Results

Using purified Topo II enzyme, we had previously reported that products formed from reactions of ˙NO and/or ˙NO-derived species with VP-16 were significantly less active than the parent drug in inducing DNA cleavage and were not cytotoxic to HL60 cells (Sinha et al., 2013). In this report, we examined whether endogenous formation of ˙NO catalyzed by iNOS in cancer cells could affect the cytotoxicity of VP-16 and Adr. To assess this, we used a human melanoma A375 tumor cell line, which has been shown to express iNOS and to produce levels of ˙NO that are relatively low (Tang and Grimm, 2004; Chanvorachote et al., 2006; Sikora et al., 2010). The presence of iNOS was confirmed in A375 cells with a primary antibody for iNOS (Fig. 1A), and our results are similar to those described previously elsewhere (Sikora et al., 2010). Furthermore, treatment of A375 cells with 10 ng/ml LPS for 18 hours significantly induced this protein, further confirming the presence of the inducible form of NOS in A375 cells (Fig. 1B). It is interesting to note that under these experimental conditions the formation of ˙NO/NO$_2$ was not detected by the Griess reaction (data not shown). This observation is similar to those previously published by Sikora et al., (2010) and Chin and Deen (2010), as the amount

of NO synthesis in A375 cells is well below (100–150 nM) the detection limits of the Griess reaction.

Examination of caspase-3 activity, a marker for apoptosis, in A375 cells showed that VP-16 alone (25 and 50 μM) induced 2.5- and 3.5-fold increases in caspase-3 activity, respectively, after 18 hours (Fig. 2A). Inhibition of iNOS with L-NIL (400 μM) further enhanced caspase-3 activity 4.5- and 6.0-fold in the presence of 25 μM and 50 μM VP-16, respectively. Consistent with these data, application of L-NIL (400 μM) significantly enhanced VP-16 cytotoxicity in A375 cells (2.5–3.5-fold; Fig. 2B). The relative IC$_{50}$ (concentration required to inhibit cell growth by 50%) is presented in Table 1. Under these conditions, L-NIL alone had no significant effect on caspase-3 activity or A375 cell viability.

Because LPS significantly induced iNOS (Fig. 1), we examined the cytotoxicity of VP-16 after induction of A375 cells with LPS. Consistent with the increase in the expression of iNOS, VP-16 cytotoxicity was further decreased in the induced A375 cells (Fig. 3A; Table 1). More interestingly, the presence of L-NIL significantly sensitized A375 cells to VP-16 (Fig. 3A; Table 1), which suggests that increased ˙NO formation from iNOS was responsible for the decrease in VP-16 cytotoxicity in A375 cells. To further examine the roles of exogenously generated ˙NO on VP-16 cytotoxicity in A375 cells, we performed coculture studies with LPS-induced macrophage RAW cells. As shown in Fig. 3B and Table 1, exogenously formed ˙NO from iNOS in RAW cells further decreased VP-16 cytotoxicity (>15-fold), suggesting that ˙NO generated from the induced RAW cells reacted with VP-16 and formed noncytotoxic species. Additionally, the data presented in Table 2 show that considerable amounts of ˙NO were generated from the induced RAW cells, and the presence of VP-16 (in coculture cytotoxicity studies) significantly decreased ˙NO formation, indicating a reaction between VP-16 and ˙NO. Furthermore, there were no significant differences in nitrite formation between the top and bottom layers (compartments) of the six-well plates, suggesting free diffusion of ˙NO across the membrane. In contrast, the cytotoxicity of VP-16 was not significantly affected (data not shown) in the presence of noninduced RAW cells, indicating that ˙NO/˙NO-species generated in the induced RAW cells from iNOS catalysis were responsible for this decrease in VP-16 cytotoxicity.

Adriamycin is a Topo II–active drug that induces protein-associated DNA damage leading to cell death, and thus it is similar to VP-16 in its mode of action. We examined the effects
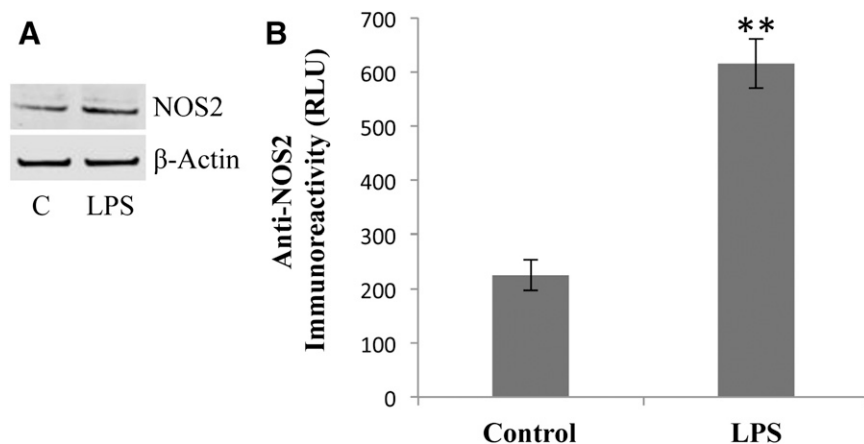
Fig. 1. (A) The Western blots for iNOS and effects of LPS (10 ng/ml) in A375 cells. (B) Quantitation of the iNOS protein in A375 cells using rabbit polyclonal anti-iNOS antibody in the standard ELISA assay as described in *Materials and Methods*. For the Western blots, A375 cells were seeded at 1×10^6 in a six-well plate. LPS (10 ng/ml) was added and exposed for 14 to 16 hours. Cells were collected, lysed, and examined for iNOS protein by Western blots. For the Western blots, 10 μg of proteins were loaded, and actin was used to assess equal loading of the proteins. Data are the mean of three separate experiments performed in duplicate. **$P < 0.005$ compared with the untreated control.

A

B
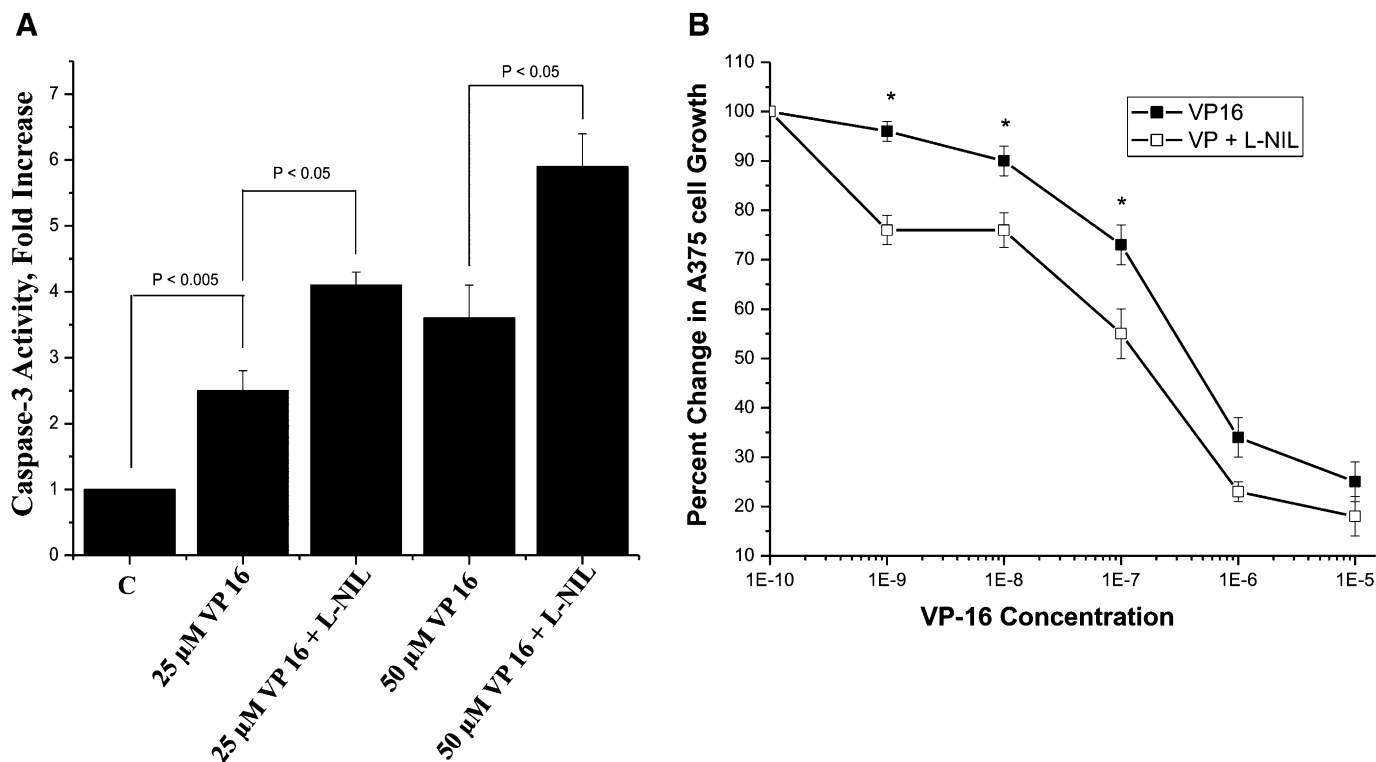
Fig. 2. (A) The caspase-3 assay as an indicator of VP-16 apoptosis in the presence or absence of iNOS inhibitors was performed according to the manufacturer's protocol. L-NIL (400 μM) was dissolved in the medium and added to A375 cells (1×10^6/well) in six-well plates and incubated for 4 hours before adding VP-16. The cells were incubated for another 18 hours before collecting cells by centrifugation. Data are the mean of three separate experiments performed in duplicate. *$P < 0.05$, $n = 3$, Student's t test. (B) Cytotoxicity studies with VP-16 in human A375 cells in the presence or absence of L-NIL (400 μM) were performed using the MTT assays described in *Materials and Methods*. Cytotoxicity data are the mean of four separate experiments performed in triplicate. *$P < 0.05$, $n = 4$, against concentration-matched VP-16 alone, Student's t test.

of endogenously generated ˙NO in Adr-induced apoptosis and cytotoxicity in A375 cells. Under similar conditions, the presence of L-NIL had no significant effects on caspase-3 activity induced by Adr (Fig. 4). Furthermore, the presence of L-NIL had no effects on the cytotoxicity of this drug (Fig. 4) in A375 cells. These observations would indicate that Adr does not react with ˙NO/˙NO-related species.

Effects of L-NIL on VP-16–Induced Cleavable Complex in A375 Cells. To determine whether iNOS catalysis influences the formation of a VP-16/Topo II complex, we evaluated the formation of the cleavage complex by VP-16 in the
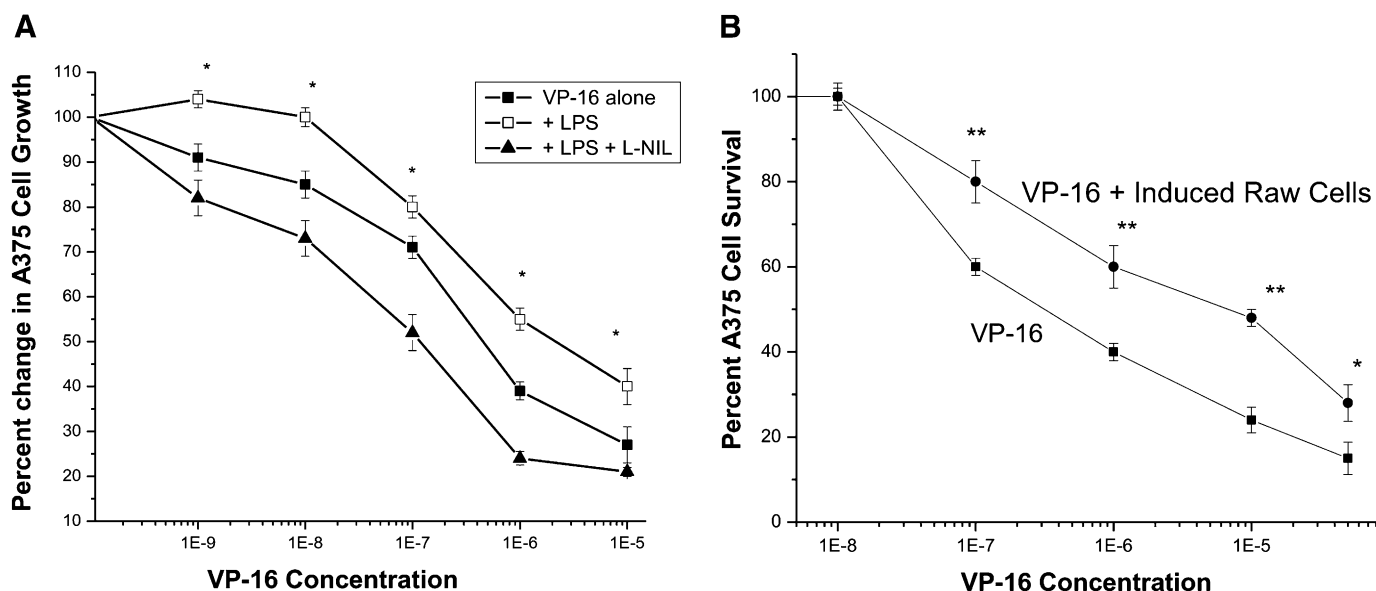
TABLE 1

Cytotoxicity of VP-16 in human A375 melanoma cells under various treatment conditions

Cytotoxicity studies were performed as described in *Materials and Methods* and also detailed in their respective figures. Data are the mean ± S.D. of three to four separate experiments.

Conditions	IC$_{50}$
	M
VP-16	$2.5 \pm 0.5 \times 10^{-7}$
VP-16 + L-NIL	$8.5 \pm 0.5 \times 10^{-8a}$
VP-16	$2.5 \pm 0.5 \times 10^{-7}$
VP-16 + LPS	$9.0 \pm 0.8 \times 10^{-7a}$
VP-16 + LPS + L-NIL	$2.0 \pm 0.5 \times 10^{-7a}$
VP-16	$5.2 \pm 0.5 \times 10^{-7}$
VP-16 + induced RAW cells	$8.5 \pm 0.70 \times 10^{-6b}$

[a] $P < 0.05$, Student's t test.
[b] $P < .005$, Student's t test.

presence of L-NIL using an SDS/KCl precipitation assay (Liu et al., 1983). As expected, treatment of A375 cells with VP-16 (10 μM) significantly increased (6- to 7-fold) the formation of the SDS/KCl precipitate (Fig. 5) over the untreated controls. The presence of L-NIL further increased this complex formation (10-fold), equivalent to the effects of VP-16 alone at 5 times the concentration (50 μM; Fig. 5). This result suggests that inhibition of ˙NO formation in A375 cells by L-NIL increased the DNA damage induced by VP-16 in a Topo II–dependent manner.

To further confirm that ˙NO or ˙NO-derived species were responsible for this decrease in VP-16–mediated Topo II–dependent DNA damage, we performed coculture experiments with induced macrophage RAW cells. Coincubation of A375 cells with induced RAW cells significantly decreased VP-16–dependent SDS-KCl precipitate formation (Fig. 5B). Similar effects were noted when the coincubations were performed either simultaneously or with preincubated VP-16 (Fig. 5B). Taken together, these observations strongly suggest that ˙NO and associated nitrogen oxides can react with VP-16, thereby making it less effective at inducing apoptosis and DNA damage and resulting in increased VP-16 resistance toward cancer cells.

Metabolism of VP-16 in A375 Melanoma Cells. To examine the effects of endogenously produced ˙NO on VP-16 metabolism in A375 cells, VP-16 was incubated with A375 cells for various times in the presence or absence of L-NIL. The HPLC analysis (Fig. 6) clearly indicated that VP-16 is rapidly metabolized in A375 cells, and a significant amount of

Fig. 3. (A) Cytotoxicity of VP-16 in A375 cells after induction with LPS (10 ng/ml 16 hours) and effects of L-NIL (400 μM) on VP-16 cytotoxicity using the MTT assay as described in Fig. 2. Data are the mean of three separate experiments performed in triplicate. *$P < 0.05$, $n = 3$, against concentration-matched VP-16 alone and VP-16 + L-NIL, Student's-t test. (B) Cytotoxicity of VP-16 in A375 cells in the presence of LPS-induced RAW cells (1×10^6 cells/incubation). Coculture studies were conducted as described in *Materials and Methods*. Data are the mean of three separate experiments performed in duplicate. *$P < 0.05$ and **$P < 0.005$, $n = 3$, against concentration-matched VP-16 alone, Student's t test.

VP-16-*o*-quinone was formed within 15 minutes of incubation. The presence of L-NIL completely inhibited the quinone formation, indicating that ˙NO and other nitric oxide species formed from iNOS in A375 cells were responsible for the *o*-quinone formation.

Discussion

The impact of NOS activity on tumor biology is diverse and dependent on a myriad of host factors (Ambs and Glynn, 2011). Likewise, ˙NO and its nitrogen oxide products can affect cancer therapy either positively or negatively (Hickok and Thomas, 2010). The present study extends our work in vitro to tumor cells and shows significant oxidative chemistry of ˙NO with VP-16.

In our previous study we showed that the reaction of ˙NO/NO species with VP-16 initiates through the obligate intermediacy of the 4′-phenoxyl radical, with subsequent formation of *o*-quinone and short-lived VP-16 nitrogen oxide species
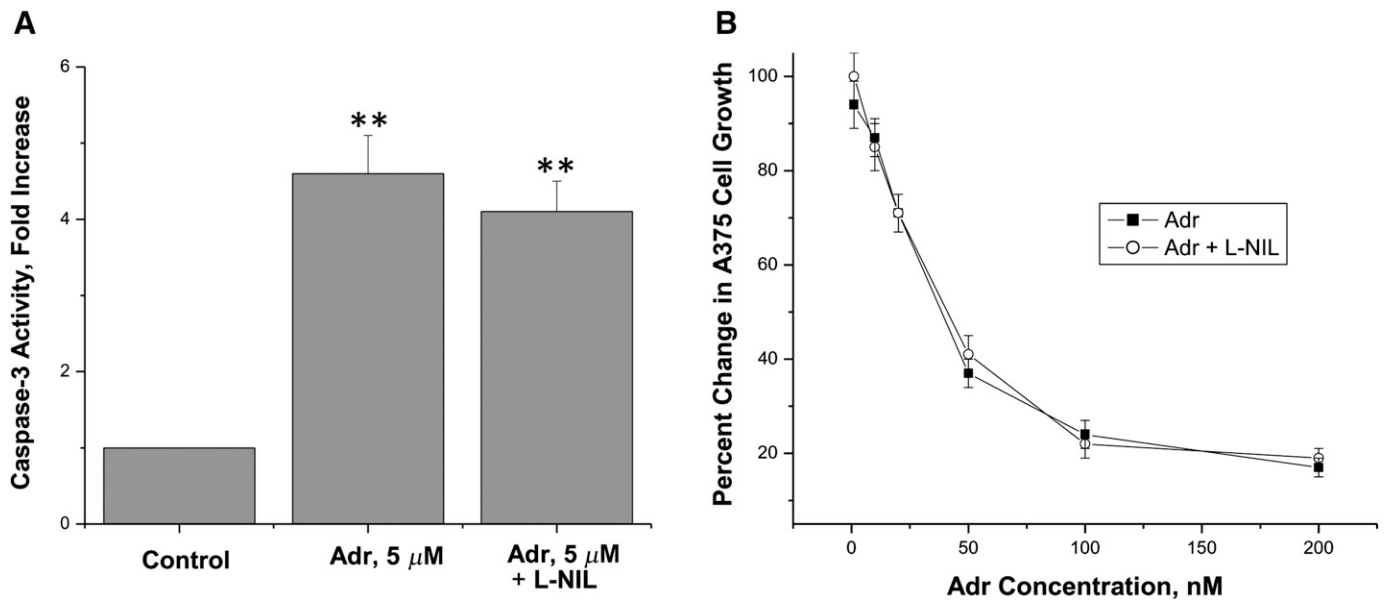
TABLE 2
Relative nitrite concentration during coculture studies for cytotoxicity with VP-16 in A375 cells in the presence of LPS-induced RAW cells

Nitrite concentrations were determined using Greiss Reagent by removing samples (100 μl; 4 hours) from the top and bottom layers (separated by 0.4 μM membrane filters; Costar, Corning, NY) in six-well plates. A375 cells were seeded in the bottom layer and the LPS-induced RAW cells were seeded on the top. The concentration of nitrite is expressed as μM/10^6 RAW cells. Data are the mean of three separate experiments.

Conditions	Top	Bottom
Control, Untreated	52.43 ± 1.0	52.32 ± 0.8
+ 50 μM VP-16	25.35 ± 2.1^a	24.7 ± 2.4^a
+ 10 μM VP-16	31.7 ± 1.6^a	25.3 ± 1.0^a
+ 1 μM VP-16	37.5 ± 1.0^a	31.8 ± 1.0^a
+ 0.1 μM VP-16	36.5 ± 1.0^b	36.7 ± 1.0^b

[a]$P < 0.005$, compared with untreated controls, Student's t test.
[b]$P < 0.05$, compared with untreated controls, Student's t test.

(Sinha et al., 2013). ˙NO reacts with phenolic compounds (Janzen et al., 1993; Yenes and Messeguer, 1999; Cudic and Ducrocq, 2000), and the initiator in these reactions is believed to be the autoxidation of ˙NO (Liu et al., 1998; Espey et al., 2001) with the formation of the ˙NO$_2$ radical, which can attack the electron-rich phenolic OH group to generate the phenoxyl radical (Hogg et al., 1996; Goss et al., 1999).

Interaction of VP-16 with Topo II has been shown to cause both single- and double-strand DNA breaks (Long et al., 1984; Glisson et al., 1986; Sinha et al., 1988), which in the absence of DNA repair results in cell death. Indeed, a significant decrease in VP-16–dependent DNA damage and cell death has been observed in cell lines where the activity of Topo II had been compromised (Glisson et al., 1986; Sinha et al., 1988). Our previous studies clearly showed that products of VP-16 exposed to ˙NO (in the presence of O$_2$) were no longer cytotoxic to HL60 cells and lacked sufficient ability to induce Topo II–dependent DNA damage (Sinha et al., 2013).

To further address the relevance of this ˙NO chemistry observed in vitro, iNOS-expressing human melanoma A375 cells were used to directly elucidate the role of ˙NO in the cytotoxicity of VP-16. Our present studies clearly show that inhibition of formation of ˙NO (and ˙NO-related species) by L-NIL increased caspase-3–dependent apoptosis by VP-16 (2-fold), with a concomitant increase (2.5- to 3.5-fold) in VP-16 cytotoxicity to A375 tumor cells (Fig. 2, A and B; Table 1). Induction of iNOS in A375 cells with LPS further decreased VP-16 cytotoxicity in A375 cells. Interestingly, inhibition of ˙NO/˙NO-related species by L-NIL resulted in sensitization of cells to VP-16. These studies taken together strongly suggest that ˙NO/˙NO-related species react with VP-16 and generate products that are significantly less cytotoxic to A375 cells.

Coculture studies performed with LPS-activated macrophage RAW cells (which generate large quantities of ˙NO/˙NO-related species) show a further (>15-fold) decrease in VP-16 cytotoxicity to A375 cells. This is a very significant finding, as

A

B

Fig. 4. Caspase-3 activity as an indicator of apoptosis (A) and cytotoxicity (B) induced by Adriamycin, respectively, in A375 cells. These studies were performed as described in Fig. 2. Data are the mean of three separate experiments performed in triplicate for the cytotoxicity and in duplicate for the caspase-3 activity. **$P < 0.005$, $n = 3$ compared with control, Student's t test.

this decrease in VP-16 cytotoxicity in the presence of exogenously generated ˙NO from macrophage cells is quite large compared with that found with endogenously generated ˙NO from iNOS catalysis in A375 cells (2.5- to 3.5-fold). Our findings would suggest that even in those cancer cells expressing low levels of iNOS, infiltrating macrophages would further increase VP-16 resistance by increasing detoxification of VP-16 via ˙NO-dependent chemistry. In tumors, the presence

of macrophages is well established, and they play significant roles in tumor progression, neovascularization, and poor survival (Jenkins et al., 1995; Lewis and Pollard, 2006; Pollard, 2008; Ambs and Glynn, 2011).

Nitric oxide has been reported to stabilize Bcl2, resulting in decreased cytotoxicity of *cis*-platinum in A375 cells (Tang and Grimm, 2004; Chanvorachote et al., 2006), thus raising the possibility of a general apoptotic resistance mechanism for

A

B
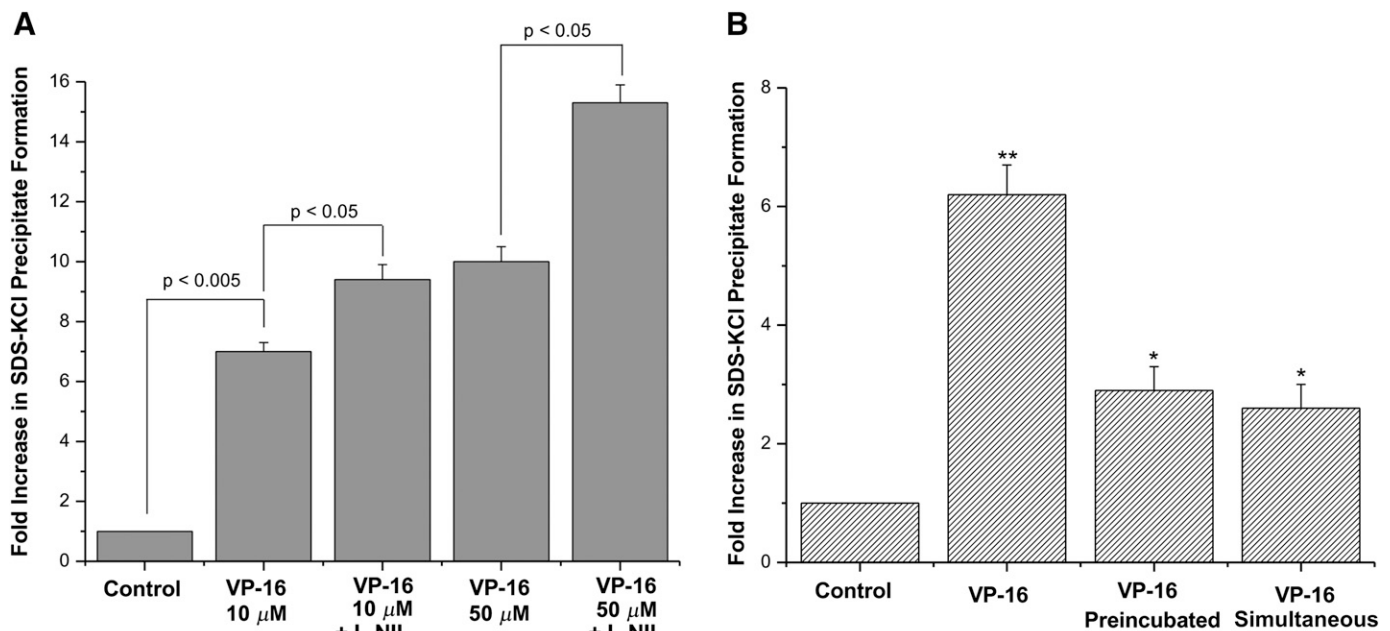
Fig. 5. (A) Measurement of the VP-16 cleavable complex formation. The SDS-KCl precipitation assay with VP-16 in the presence of L-NIL was performed as described in *Materials and Methods*. L-NIL (400 μM) was incubated with the cells for 18 hours during the labeling phase before VP-16 was added for 1 hour. * $P < 0.05$, $n = 3$ compared with controls and 10 μM VP-16 treatment and 50 μM + L-NIL treatment compared with 50 μM VP-16 treatment alone. (B) Coculture experiments for determination of SDS-KCl precipitate formation were performed with LPS-induced (1 μg/ml for 14–16 hours) RAW cells as described in *Materials and Methods*. **$P < 0.005$, $n = 3$, compared with control and VP-16 treated simultaneously or preincubated; *$P < 0.05$, $n = 3$ compared with control), Student's t test.
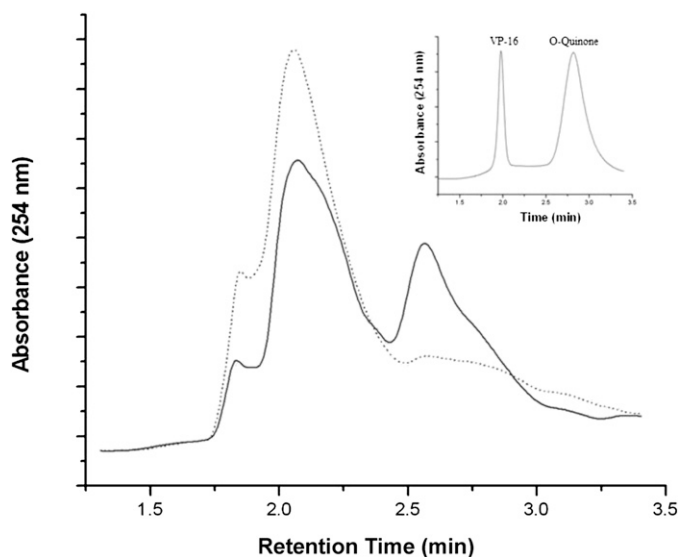
Fig. 6. HPLC analysis of the cellular metabolism of VP-16 (100 μM) in the presence or absence of L-NIL (400 μM). A375 cells were incubated with L-NIL for 18 hours before VP-16 was added and incubated for 15 minutes afterward. Metabolites were isolated as described in *Materials and Methods* and analyzed by HPLC. The solid line represents cells treated with VP-16 only, and the dashed line represents cells treated with both VP-16 and L-NIL. Insert: The HPLC analysis of products formed in vitro during reactions of ·NO gas with VP-16 at a low ratio in chloroform, as described elsewhere (Sinha et al., 2013).

·NO independent of direct VP-16 reactions. However, our current study shows that endogenously/exogenously formed ·NO (or ·NO-derived species) reacts with VP-16 to generate less active metabolites of VP-16, resulting in a decrease in both Topo II–mediated DNA damage and cytotoxicity. In contrast, L-NIL had no significant effects on Adr-induced apoptosis or cytotoxicity in A375 cells, which would indicate that Bcl2 did not play a role in VP-16 activity.

Inhibition of cellular ·NO formation by L-NIL caused an increase in intracellular unmodified VP-16, resulting in increased DNA damage and cytotoxicity. Our observations with Adr further confirm that L-NIL did not affect apoptosis nor did it significantly affect its cytotoxicity. Similar observations were also noted with Camptothecin, a Topo I–active drug, where the presence of L-NIL had no significant effect on caspase-3 activity or its cytotoxicity in A375 cells (unpublished observations), lending support to the conclusion that L-NIL did not modulate VP-16 pharmacology by nonspecific effects on caspase-3 or Topo II activities. We conclude, therefore, that iNOS catalysis within A375 tumor cells was sufficient to directly detoxify active VP-16 via ·NO/·NO$_2$-dependent oxidative reactions.

·NO readily partitions into a hydrophobic medium, such as the interior of membranes (Liu et al., 1998). This, in combination with a relatively high rate of ·NO generation from iNOS catalysis, facilitates ·NO autoxidation and formation of ·NO$_2$ (Hogg et al., 1996; Goss et al., 1999; Moller et al., 2007). The organic solubility of VP-16 may likewise localize and enhance interactions with reactive nitrogen oxides. The occurrence of both augmented iNOS catalysis (Ambs and Glynn, 2011) and alterations in cancer cell plasma membrane architecture (Zhuang et al., 2002; Moller et al., 2007; Miersch et al., 2008) will significantly influence iNOS-dependent detoxification of VP-16 and resistance toward cancer cells.

While in human patients VP-16 is exclusively metabolized by Cyp3A4 in the liver to its dihydroxy derivative, it is possible that VP-16 could also be metabolized by Cyp3A4 in A375 melanoma cells to the catechol derivative and *o*-quinone. The roles of Cyp3A4 in A375 cells were not investigated in our present study, but inhibition of *o*-quinone formation by L-NIL would suggest that ·NO was involved in its formation in A375 cells. The formation of the *o*-quinone was rapid and decreased significantly with time, suggesting binding to proteins and DNA. The formation of VP-16-*o*-quinone by ·NO-dependent pathways is very significant in light of the role of the quinone in the induction of acute myeloid leukemia in patients treated with VP-16. It has been reported that VP-16 metabolites increase Topo II–dependent cleavage near leukemia-associated MLL translocation breakpoints (Lovett et al., 2001). Furthermore, Vlasova et al. (2011) have shown that the VP-16 radical formed from 1-electron oxidation can redox cycle, leading to enhanced Topo II–mediated strand breaks and MLL gene translocation. Our previous studies have shown that VP-16 is readily oxidized by ·NO chemistry to its phenoxyl radical, an obligatory intermediate in the formation of the VP-16-*o*-quinone (Sinha et al., 2013).

We conclude from our findings that ·NO oxidative chemistry occurs in A375 cancer cells and can detoxify VP-16. Our results provide insight into the pharmacology and anticancer activities of VP-16 in tumors that may ultimately contribute to increased resistance and treatment failure. VP-16 is currently used for the treatment of a variety of cancers (e.g., lung, melanoma, and breast) that are known to express iNOS (Chen et al., 2008; Grimm et al., 2008). It is tempting to suggest that the use of VP-16 and related anticancer drugs capable of reacting with ·NO/·NO$_2$ may be ill-advised for patients harboring cancers with intensive iNOS activity. Furthermore, in tumors that do not express significant amounts of iNOS, infiltrating macrophages may further detoxify VP-16 and render tumor cells resistant to VP-16, as shown in our studies with melanoma cells.

Authorship Contributions

Participated in research design: Sinha, Kumar, Bhattacharjee, Mason.

Conducted experiments: Sinha, Kumar, Bhattacharjee

Contributed to new reagents or analytic tools: Kumar, Bhattacharjee.

Performed data analysis: Sinha, Kumar, Bhattacharjee, Espey.

Wrote or contributed to writing of the manuscript: Sinha, Mason.

References

Alley MC, Scudiero DA, Monks A, Hursey ML, Czerwinski MJ, Fine DL, Abbott BJ, Mayo JG, Shoemaker RH, and Boyd MR (1988) Feasibility of drug screening with panels of human tumor cell lines using a microculture tetrazolium assay. *Cancer Res* 48:589–601.

Ambs S and Glynn SA (2011) Candidate pathways linking inducible nitric oxide synthase to a basal-like transcription pattern and tumor progression in human breast cancer. *Cell Cycle* 10:619–624.

Chatterjee S, Lardinois O, Bonini MG, Bhattacharjee S, Stadler K, Corbett J, Deterding LJ, Tomer KB, Kadiiska M, and Mason RP (2009) Site-specific carboxypeptidase B1 tyrosine nitration and pathophysiological implications following its physical association with nitric oxide synthase-3 in experimental sepsis. *J Immunol* 183:4055–4066.

Chanvorachote P, Nimmannit U, Stehlik C, Wang L, Jiang BH, Ongpipatanakul B, and Rojanasakul Y (2006) Nitric oxide regulates cell sensitivity to cisplatin-

induced apoptosis through S-nitrosylation and inhibition of Bcl-2 ubiquitination. *Cancer Res* **66**:6353–6360.

Chen GG, Lee TW, Xu H, Yip JHY, Li M, Mok TSK, and Yim AP (2008) Increased inducible nitric oxide synthase in lung carcinoma of smokers. *Cancer* **112**:372–381.

Chin MP and Deen WM (2010) Prediction of nitric oxide concentrations in melanoma. *Nitric Oxide* **23**:319–326.

Cook JA, Krishna MC, Pacelli R, DeGraff W, Liebmann J, Mitchell JB, Russo A, and Wink DA (1997) Nitric oxide enhancement of melphalan-induced cytotoxicity. *Br J Cancer* **76**:325–334.

Cudic M and Ducrocq C (2000) Transformations of 2,6-diisopropylphenol by NO-derived nitrogen oxides, particularly peroxynitrite. *Nitric Oxide* **4**:147–156.

Curtis JF, Reddy NG, Mason RP, Kalyanaraman B, and Eling TE (1996) Nitric oxide: a prostaglandin H synthase 1 and 2 reducing cosubstrate that does not stimulate cyclooxygenase activity or prostaglandin H synthase expression in murine macrophages. *Arch Biochem Biophys* **335**:369–376.

Doroshow JH (1983) Anthracycline antibiotic-stimulated superoxide, hydrogen peroxide, and hydroxyl radical production by NADH dehydrogenase. *Cancer Res* **43**:4543–4551.

Espey MG, Miranda KM, Thomas DD, and Wink DA (2001) Distinction between nitrosating mechanisms within human cells and aqueous solution. *J Biol Chem* **276**:30085–30091.

Evig CB, Kelley EE, Weydert CJ, Chu Y, Buettner GR, and Burns CP (2004) Endogenous production and exogenous exposure to nitric oxide augment doxorubicin cytotoxicity for breast cancer cells but not cardiac myoblasts. *Nitric Oxide* **10**:119–129.

Fan Y, Schreiber EM, Giorgianni A, Yalowich JC, and Day BW (2006) Myeloperoxidase-catalyzed metabolism of etoposide to its quinone and glutathione adduct forms in HL60 cells. *Chem Res Toxicol* **19**:937–943.

Gantchev TG and Hunting DJ (1998) The ortho-quinone metabolite of the anticancer drug etoposide (VP-16) is a potent inhibitor of the topoisomerase II/DNA cleavable complex. *Mol Pharmacol* **53**:422–428.

Glisson B, Gupta R, Smallwood-Kentro S, and Ross WE (1986) Characterization of acquired epipodophyllotoxin resistance in a Chinese hamster ovary cell line: loss of drug-stimulated DNA cleavage activity. *Cancer Res* **46**:1934–1938.

Goss SPA, Singh RJ, Hogg N, and Kalyanaraman B (1999) Reactions of *NO, *NO2 and peroxynitrite in membranes: physiological implications. *Free Radic Res* **31**:597–606.

Grimm EA, Ellerhorst J, Tang CH, and Ekmekcioglu S (2008) Constitutive intracellular production of iNOS and NO in human melanoma: possible role in regulation of growth and resistance to apoptosis. *Nitric Oxide* **19**:133–137.

Haim N, Roman J, Nemec J, and Sinha BK (1986) Peroxidative free radical formation and *O*-demethylation of etoposide (VP-16) and teniposide (VM-26). *Biochem Biophys Res Commun* **135**:215–220.

Haim N, Nemec J, Roman J, and Sinha BK (1987a) In vitro metabolism of etoposide (VP-16-213) by liver microsomes and irreversible binding of reactive intermediates to microsomal proteins. *Biochem Pharmacol* **36**:527–536.

Haim N, Nemec J, Roman J, and Sinha BK (1987b) Peroxidase-catalyzed metabolism of etoposide (VP-16-213) and covalent binding of reactive intermediates to cellular macromolecules. *Cancer Res* **47**:5835–5840.

Henwood JM and Brogden RN (1990) Etoposide. A review of its pharmacodynamic and pharmacokinetic properties, and therapeutic potential in combination chemotherapy of cancer. *Drugs* **39**:438–490.

Hickok JR and Thomas DD (2010) Nitric oxide and cancer therapy: the emperor has NO clothes. *Curr Pharm Des* **16**:381–391.

Hogg N, Singh RJ, Goss SPA, and Kalyanaraman B (1996) The reaction between nitric oxide and alpha-tocopherol: a reappraisal. *Biochem Biophys Res Commun* **224**:696–702.

Jenkins DC, Charles IG, Thomsen LL, Moss DW, Holmes LS, Baylis SA, Rhodes P, Westmore K, Emson PC, and Moncada S (1995) Roles of nitric oxide in tumor growth. *Proc Natl Acad Sci USA* **92**:4392–4396.

Janzen EG, Wilcox AL, and Manoharan V (1993) Reactions of nitric oxide with phenolic antioxidants and phenoxyl radicals. *J Org Chem* **58**:3597–3599 DOI: 10.1021/jo00066a001.

Kagan VE, Kuzmenko AI, Tyurina YY, Shvedova AA, Matsura T, and Yalowich JC (2001) Pro-oxidant and antioxidant mechanisms of etoposide in HL-60 cells: role of myeloperoxidase. *Cancer Res* **61**:7777–7784.

Kalyanaraman B, Perez-Reyes E, and Mason RP (1980) Spin-trapping and direct electron spin resonance investigations of the redox metabolism of quinone anticancer drugs. *Biochim Biophys Acta* **630**:119–130.

Kalyanaraman B, Nemec J, and Sinha BK (1989) Characterization of free radicals produced during oxidation of etoposide (VP-16) and its catechol and quinone derivatives. An ESR Study. *Biochemistry* **28**:4839–4846.

Katki AG, Kalyanaraman B, and Sinha BK (1987) Interactions of the antitumor drug, etoposide, with reduced thiols in vitro and in vivo. *Chem Biol Interact* **62**:237–247.

Lewis CE and Pollard JW (2006) Distinct role of macrophages in different tumor microenvironments. *Cancer Res* **66**:605–612.

Lepoivre M, Flaman JM, Bobé P, Lemaire G, and Henry Y (1994) Quenching of the tyrosyl free radical of ribonucleotide reductase by nitric oxide. Relationship to cytostasis induced in tumor cells by cytotoxic macrophages. *J Biol Chem* **269**:21891–21897.

Liu LF (1989) DNA topoisomerase poisons as antitumor drugs. *Annu Rev Biochem* **58**:351–375.

Liu LF, Rowe TC, Yang L, Tewey KM, and Chen GL (1983) Cleavage of DNA by mammalian DNA topoisomerase II. *J Biol Chem* **258**:15365–15370.

Liu X, Miller MJ, Joshi MS, Thomas DD, and Lancaster JR, Jr (1998) Accelerated reaction of nitric oxide with O2 within the hydrophobic interior of biological membranes. *Proc Natl Acad Sci USA* **95**:2175–2179.

Loike JD and Horwitz SB (1976) Effect of VP-16-213 on the intracellular degradation of DNA in HeLa cells. *Biochemistry* **15**:5443–5448.

Long BH, Musial ST, and Brattain MG (1984) Comparison of cytotoxicity and DNA breakage activity of congeners of podophyllotoxin including VP16-213 and VM26: a quantitative structure-activity relationship. *Biochemistry* **23**:1183–1188.

Lovett BD, Strumberg D, Blair IA, Pang SK, Burden DA, Megonigal MD, Rappaport EF, Rebbeck TR, Osheroff N, and Pommier YG, et al. (2001) Etoposide metabolites enhance DNA topoisomerase II cleavage near leukemia-associated MLL translocation breakpoints. *Biochemistry* **40**:1159–1170.

Miersch S, Espey MG, Chaube R, Akarca A, Tweten R, Ananvoranich S, and Mutus B (2008) Plasma membrane cholesterol content affects nitric oxide diffusion dynamics and signaling. *J Biol Chem* **283**:18513–18521.

Möller MN, Li Q, Vitturi DA, Robinson JM, Lancaster JR, Jr, and Denicola A (2007) Membrane "lens" effect: focusing the formation of reactive nitrogen oxides from the *NO/O2 reaction. *Chem Res Toxicol* **20**:709–714.

Myers CE, Mimnuagh E, Yeh G, and Sinha BK (1987) *Biochemical Mechanism of Tumor Cell Kill by the Anthracyclines in Anthracyclines and Anthracenedione-Based Anticancer Agents* (Lown W, ed) pp 527–569, Elsevier, NY.

Pollard JW (2008) Macrophages define the invasive microenvironment in breast cancer. *J Leukoc Biol* **84**:623–630.

Rajagopalan S, Politi PM, Sinha BK, and Myers CE (1988) Adriamycin-induced free radical formation in the perfused rat heart: implications for cardiotoxicity. *Cancer Res* **48**:4766–4769.

Ranguelova K, Suarez J, Magliozzo RS, and Mason RP (2008) Spin trapping investigation of peroxide- and isoniazid-induced radicals in *Mycobacterium tuberculosis* catalase-peroxidase. *Biochemistry* **47**:11377–11385.

Sikora AG, Gelbard A, Davies MA, Sano D, Ekmekcioglu S, Kwon J, Hailemichael Y, Jayaraman P, Myers JN, and Grimm EA, et al. (2010) Targeted inhibition of inducible nitric oxide synthase inhibits growth of human melanoma in vivo and synergizes with chemotherapy. *Clin Cancer Res* **16**:1834–1844.

Sinha BK (1995) Topoisomerase inhibitors: therapeutic potentials. *Drugs* **49**:11–19.

Sinha BK, Politi PM, Eliot HM, Kerrigan D, and Pommier Y (1990) Structure-activity relations, cytotoxicity and topoisomerase II dependent cleavage induced by pendulum ring analogues of etoposide. *Eur J Cancer* **26**:590–593.

Sinha BK (1980) Binding specificity of chemically and enzymatically activated anthracycline anticancer agents to nucleic acids. *Chem Biol Interact* **30**:67–77.

Sinha BK, Trush MA, Kennedy KA, and Mimnaugh EG (1984) Enzymatic activation and binding of adriamycin to nuclear DNA. *Cancer Res* **44**:2892–2896.

Sinha BK, Katki AG, Batist G, Cowan KH, and Myers CE (1987) Differential formation of hydroxyl radicals by Adriamycin in sensitive and resistant MCF-7 human breast tumor cells: implications for the mechanism of action. *Biochemistry* **26**:3776–3781.

Sinha BK, Haim N, Dusre L, Kerrigan D, and Pommier Y (1988) DNA strand breaks produced by etoposide (VP-16,213) in sensitive and resistant human breast tumor cells: implications for the mechanism of action. *Cancer Res* **48**:5096–5100.

Sinha BK, Bhattacharjee S, Chatterjee S, Jiang JJ, Motten AG, Kumar A, Espey MG, and Mason RP (2013) Role of nitric oxide in the chemistry and anticancer activity of etoposide (VP-16,213). *Chem Res Toxicol* **26**:379–387.

Tang CH and Grimm EA (2004) Depletion of endogenous nitric oxide enhances cisplatin-induced apoptosis in a p53-dependent manner in melanoma cell lines. *J Biol Chem* **279**:288–298.

Wink DA, Cook JA, Christodoulou D, Krishna MC, Pacelli R, Kim S, Degraff W, Gamsom J, Vodovotz Y, and Russo A, et al. (1997) Nitric oxide and some NO donor compounds enhance the cytotoxicity of cisplatin. *Nitric Oxide* **1**:88–94.

Wink DA, Vodovotz Y, Cook JA, Krishna MC, Kim S, Coffin D, DeGraff W, Deluca AM, Liebmann J, and Mitchell JB (1998) The role of nitric oxide chemistry in cancer treatment. *Biochemistry (Mosc)* **63**:802–809.

van Maanen JMS, de Vries J, Pappie D, van den Akker E, Lafleur VM, Retèl J, van der Greef J, and Pinedo HM (1987) Cytochrome P-450-mediated O-demethylation: a route in the metabolic activation of etoposide (VP-16-213). *Cancer Res* **47**:4658–4662.

Vlasova II, Feng W-H, Goff JP, Giorgianni A, Do D, Gollin SM, Lewis DW, Kagan VE, and Yalowich JC (2011) Myeloperoxidase-dependent oxidation of etoposide in human myeloid progenitor CD34+ cells. *Mol Pharmacol* **79**:479–487.

Xu WM, Liu LZ, Loizidou M, Ahmed M, and Charles IG (2002) The role of nitric oxide in cancer. *Cell Res* **12**:311–320.

Yenes S and Messeguer A (1999) A study of the reaction of different phenol substrates with nitric oxide and peroxynitrite. *Tetrahedron* **55**:14111–14122 DOI: 10.1016/S0040-4020(99)00877-7.

Zhuang L, Lin JQ, Lu ML, Solomon KR, and Freeman MR (2002) Cholesterol-rich lipid rafts mediate akt-regulated survival in prostate cancer cells. *Cancer Res* **62**:2227–2231.

Address correspondence to: Dr. Birandra K. Sinha, National Institutes of Environmental Health Sciences, Research Triangle Park, North Carolina 27709. E-mail: sinha1@niehs.nih.gov